INT. J. REMOTE SENSING, 10 OCTOBER, 2004,
VOL. 25, NO. 19, 4051–4059

Taylor & Francis
Taylor & Francis Group

Masking turbid water in the southeastern Mediterranean Sea utilizing the SeaWiFS 510 nm spectral band

D. FIGUERAS†‡, A. KARNIELI†*, A. BRENNER‡ and Y. J. KAUFMAN§

†The Remote Sensing Laboratory, Jacob Blaustein Institute for Desert Research, Ben Gurion University of the Negev, Sede Boker Campus, 84990, Israel
‡Department of Environmental Engineering, Ben Gurion University of the Negev, Beer Sheva 84105, Israel
§NASA Goddard Space Flight Center, Greenbelt, MD 20771, USA

(*Received 26 June 2001; in final form 12 November 2003*)

Abstract. A simplified model for masking water turbidity in the southeastern Mediterranean Sea is suggested and demonstrated using SeaWiFS images. The model is implemented by using a null point at 497 nm (corresponding to SeaWiFS band 4 centred at 510 nm) where the level of reflectance is not affected by change in chlorophyll concentration. Any shift of reflectance above the null point indicates suspended matter present in the water. Masking of pixels with values above the threshold results in elimination of the turbidity. The 510 nm null point can also be used for calculating suspended matter concentrations in the area, since it defines the effects of suspended matter on the spectrum.

1. Introduction

The accurate measurement of chlorophyll-*a* (CHL) concentration in coastal areas is problematic and affected by an almost unlimited number of substances of anthropogenic and inland origin present in the water. These substances affect the spectral radiance along the entire visible range. The main components of coastal waters are usually coloured dissolved organic matter (CDOM) and suspended matter (SM). The latter shifts the spectrum towards longer wavelengths (Bukata *et al*. 1983, Bhargava and Mariam 1990).

The Sea-Viewing Wide-Field-of-View Sensor (SeaWiFS) is a spaceborne instrument for measuring radiance in specific spectral bands of the visible spectrum (http://seawifs.gsfc.nasa.gov/SEAWIFS/SEASTAR/SPACECRAFT.html). The measured radiance is related quantitatively to various constituents in the water column, such as CHL, SM, and CDOM (table 1), which interact with the visible spectrum. The SeaWiFS Data Analysis System (SeaDAS) is a comprehensive image analysis package, developed by NASA, for the processing, display, and analysis of SeaWiFS

*Corresponding author; e-mail: karnieli@bgumail.bgu.ac.il

International Journal of Remote Sensing
ISSN 0143-1161 print/ISSN 1366-5901 online © 2004 Taylor & Francis Ltd
http://www.tandf.co.uk/journals
DOI: 10.1080/01431160310001657498

Table 1. SeaWiFS spectral bands and primary use.

Band	Centre wavelength (nm)	Colour	Primary use
1	412	violet	Dissolved organic matter (including Gelbstoffe)
2	443	blue	Chlorophyll absorption
3	490	blue-green	Pigment absorption (Case II), K(490)
4	510	blue-green	Chlorophyll absorption
5	555	green	Pigments, optical properties, sediments
6	670	red	Atmospheric correction
7	765	near IR	Atmospheric correction, aerosol radiance
8	865	near IR	Atmospheric correction, aerosol radiance

and other sensor data (McClain *et al.* 1995, http://seadas.gsfc.nasa.gov). The program incorporates various algorithms for creating different products.

Algorithms for computing CHL concentrations (C_{CHL}), such as the SeaWiFS OC4V4 (O'Reilly *et al.* 2000, equation (1)), were composed initially for application in the open, deep sea, denoted as Case I water (Morel and Prieur 1977):

$$C_{\mathrm{CHL}} = 10^{\left(0.366 - 3.067R + 1.930R^2 + 0.649R^3 - 1.532R^4\right)} \tag{1}$$

where the reflectance R is defined as

$$R = \log_{10}\left(R_{555}^{443} > R_{555}^{490} > R_{555}^{510}\right) \tag{2}$$

This algorithm has been applied mainly for understanding the carbon cycle, spotting large fish schools for the fish industry, etc. Anthropogenic induced substances and sediments are not present in the open ocean in sufficient concentrations to influence the spectral characteristics of the water (Morel and Prieur 1977, Nanu 1993). Therefore, standard CHL algorithms introduce erroneous CHL concentrations in Case II areas.

The SeaDAS program also contains an algorithm for masking turbid water based on Bricaud and Morel (1987). The condition for limiting reflectance for Case I water at 555 nm is expressed as $R_{\mathrm{lim}}(555)$, using SeaWiFS channel 5 and applying multiple variables such as the diffuse attenuation coefficient for downwelling irradiance (K_{d}), backscattering coefficient (b_{b}), index of refraction ($n = 1.341$), Fresnel reflectivity (ρ), and the additional SeaDAS chlorophyll and phaeopigment algorithms:

$$R_{\mathrm{lim}}(555) = \frac{1 - 2.5B - \sqrt{\left((2.5B-1)^2 - 4.44B\right)}}{2} \tag{3}$$

$$B = 0.33 b_{\mathrm{b}} / K_{\mathrm{d}} \tag{4}$$

$$b_{\mathrm{b}}(555) = 0.00075 + [0.0063 - 0.00263\log(C_{\mathrm{CHL}})] {C_{\mathrm{CHL}}}^{0.62} \tag{5}$$

$$K_{\mathrm{d}}(555) = 0.0717 + 0.039 {C_{\mathrm{CHL}}}^{0.64} \tag{6}$$

where C_{CHL} is the pigment concentration based on the SeaDAS algorithm (equation (1)). The remote sensing reflectance (R_{RS}) is a SeaWiFS product defined as the ratio between normalized water leaving radiance (nlw) and extraterrestrial solar reflectance (F_0) for any specific spectral band (λ):

$$R_{\mathrm{RS}} = nlw / F_0 \tag{7}$$

The turbid water mask is set when R_{RS} exceeds a value analogous to R_{lim}, i.e.

$$R_{RS}(555) > (1-\rho)R_{lim}(555)/Qn^2 \quad (8)$$

where $Q = 3.42$ is defined as the ratio of upwelling irradiance to radiance that varies with the angular distribution of the upwelling light field, and is equal to π for an isotropic distribution. Despite the complexity of the above procedure, it is not intended to remove the effects of turbid water from the CHL product in order to recognize solely the CHL.

The objective of the current project was to develop a simplified and efficient algorithm for removing the effect of SM in the SeaWIFS CHL product. The proposed algorithm was tested and demonstrated on the southeastern Mediterranean Sea where both SM and CHL are present in the water.

2. Material and methods

SeaWiFS images were acquired at the high resolution picture transmission (HRPT) receiving station at Sede Boker Campus, Israel. Image processing was performed using the SeaDAS image analysis program, on Level-2 GAC Data Products (http://seawifs.gsfc.nasa.gov/SEAWIFS/SOFTWARE/DATA_PRODUCTS.html). The main data contents of this product are the geophysical values for each pixel, derived from the Level-1A raw radiance counts by applying the sensor calibration, atmospheric corrections, and bio-optical algorithms. The OC4V4 CHL algorithm was applied to 220 SeaWiFS images from the years 2000–2001.

3. Detecting and masking SM in water

The OC4V4 algorithm recognizes a large area near the coast of Egypt by the Nile Delta as having extremely high CHL concentrations—above $60\,mg\,m^{-3}$ (figure 1(*a*)). However, this area is known to have high concentrations of sediments from Nilotical sources, originating from the Nile Delta and transported eastwards by the geostrophic circum-Mediterranean cyclonic gyre, derived by the regional dominant winds (Emery and Neev 1970, Karnieli *et al.* 1993, Mayo *et al.* 1993, Gitelson *et al.* 1996).

Due to the above erroneous CHL values, a model for estimating SM concentrations was needed to detect and mask all suspended sediments in the study area. A few models were examined—Tassan (1981), Froidefont *et al.* (2002), and Mayo *et al.* (1993). The latter was implemented for the southeastern Mediterranean Sea and is presented in figure 1(*b*). Note the similarity in CHL and SM distributions on both products.

The current proposed method is based on the fact that at the 497 nm wavelength, CHL concentrations do not affect the upwelling water-leaving radiance, on condition that the water is pure and there is no SM or CDOM present (Bukata *et al.* 1995). Consequently, a threshold for distinguishing between CHL and SM will be the R_{RS} value at 497 nm of Case I water. On implementing this 'null point' procedure on water with the presence of SM additional to CHL, every shift of the spectrum above this point should be a result of SM present in the water body.

The above hypothesis is demonstrated hereby on an image of 18 June 2001 (figure 1(*a*)). High CHL concentrations were detected throughout the southeastern Mediterranean coastline. Maximal concentrations, north of the Nile delta, computed by OC4V4, reached $61.71\,mg\,m^{-3}$. Average pelagic concentrations were $0.07\,mg\,m^{-3}$. Average concentrations 60 km west of the coast offshore the Tel Aviv area, where high loads of nutrients are discharged daily, reached $1.41\,mg\,m^{-3}$.

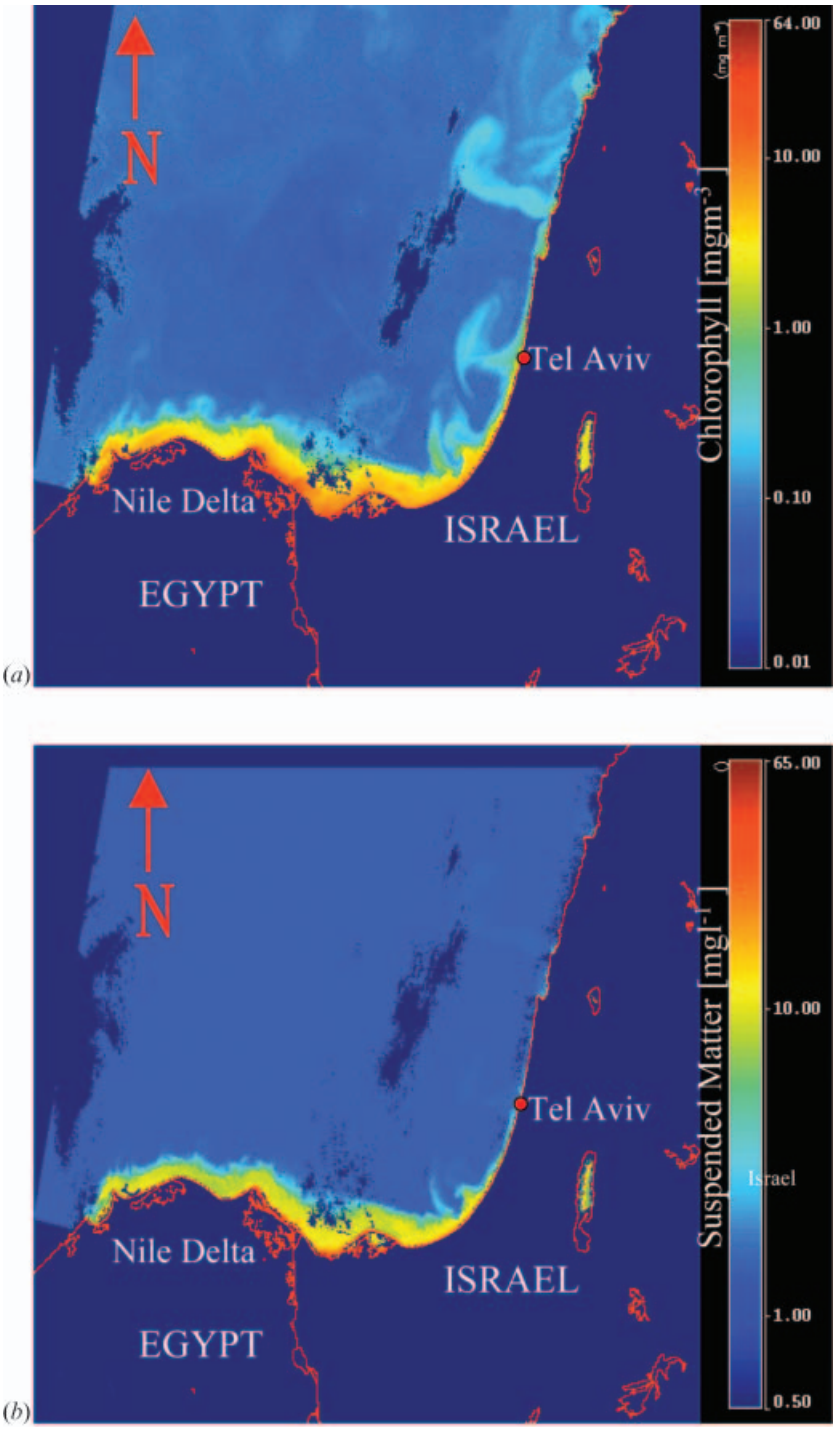

Figure 1. SeaWiFS products demonstrated on image of 18 June 2001 of the southeastern Mediterranean: (*a*) suspended matter concentration based on Mayo *et al.* (1993) model; (*b*) chlorophyll-*a* concentration based on O'Reilly *et al.* (2000) OC4V4 model. Both products detect high signals along the Egyptian coasts but interpret them differently.

Using the SeaDAS turbid water mask, spectral data from Case I and II areas were collected and analysed.

4. Case I areas

Suspended matter concentrations in Case I areas west of the Israeli coastline were negligible (Herut *et al.* 1999). In order to validate this statement, a total of 1175 pixels ($\sim 1175\,km^2$) from several representative images, from different seasons, were examined in an open-sea area between Egypt, Israel, and Cyprus. Results show that average CHL concentrations, according to OC4V4 model, varied between 0.09 to $0.27\,mg\,m^{-3}$. The null point (figure 2(*a*)) is located between SeaWiFS channels 3 and 4 ($\lambda = 490$ and $\lambda = 510\,nm$, respectively). The minimum coefficient of variation (CV) in the visible spectrum (412–670 nm) was calculated to select the reference band for chlorophyll. The lowest CV was found at the $\lambda = 510\,nm$ wavelength (figure 3) where $CV = 0.11$ corresponds to average $R_{RS} = 0.0039$.

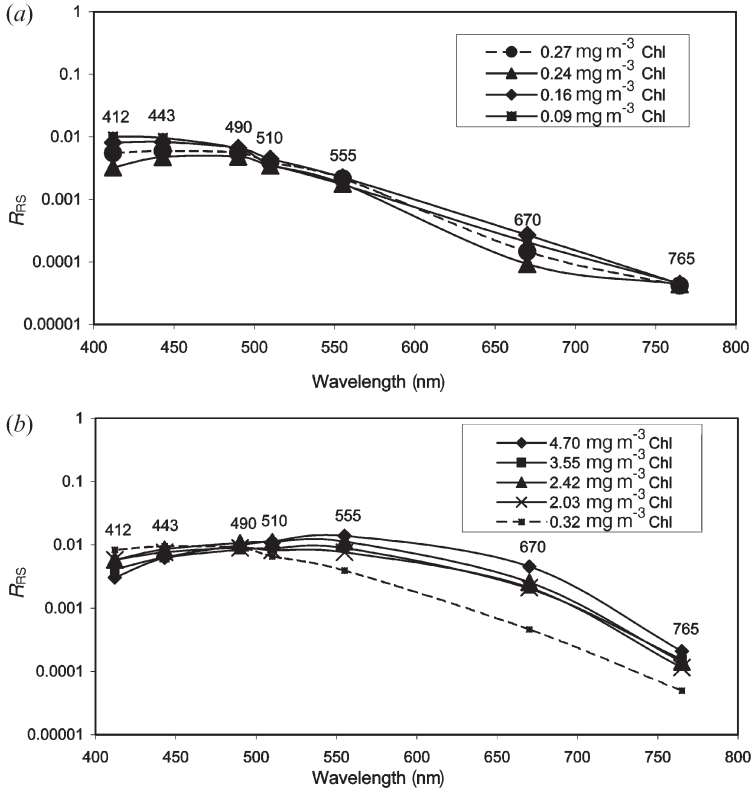

Figure 2. Volume reflectance spectra in a (*a*) Case I pelagic environment; (*b*) Case II environment containing different sediment concentrations offshore from the Nile Delta. Volume reflectance spectra of the Case II water show larger values than those of the Case I water in all SeaWiFS bands due to high suspended matter concentrations.

5. Case II areas

A total of 1006 pixels ($\sim 1006\,km^2$) from several representative images were examined offshore from the Nile Delta (Case II water), where water contains high sediment concentrations (figure 1). Volume reflectance spectra show larger values than in the Case I water in all SeaWiFS bands due to high SM concentrations. CHL concentrations (OC4V4 model) vary between 0.32 and $4.70\,mg\,m^{-3}$. The location of the null point is the 490 nm wavelength, corresponding to CV = 0.09 (figure 3).

6. SM classification

Mayo *et al.* (1993) demonstrated a large correlation between the CZCS 520 nm band and SM concentration in the Nile delta area. According to the present model, any result higher than the reference point, at 510 nm, represents a shift caused by SM, and therefore this area will be classified as Case II water. The calculation for

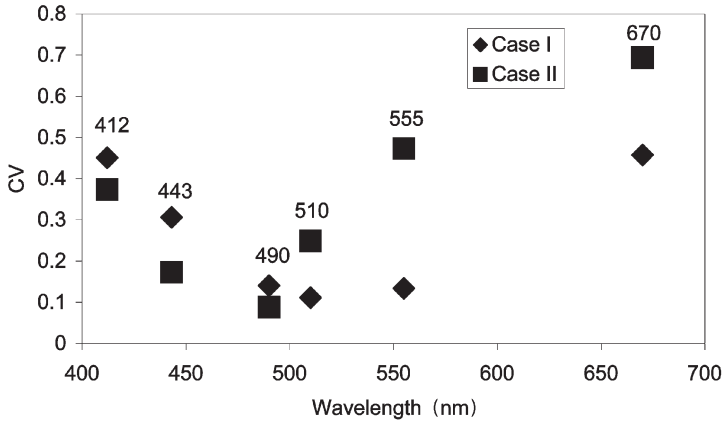

Figure 3. Coefficient of variation (CV) of R_{RS} measured offshore from the Nile Delta (Case II) and in the pelagic waters of the southeastern Mediterranean (Case I). Lowest CV value of Case I water corresponds to SeaWiFS 510 nm spectral band.

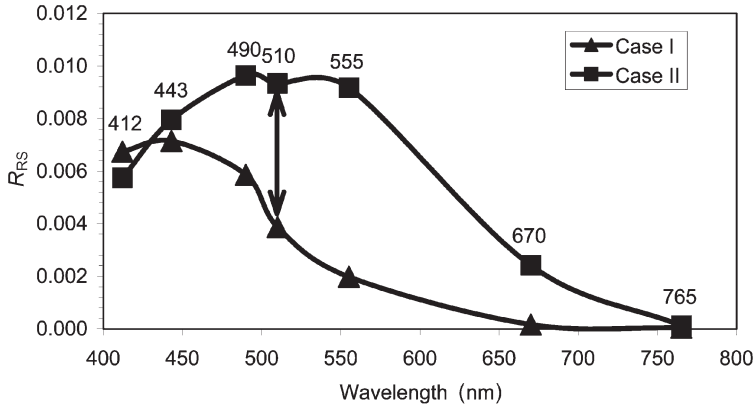

Figure 4. Volume reflectance spectra featuring the relative contribution of water turbidity to reflectance at the 510 nm wavelength in relation to chlorophyll-*a*. Arrow represents shift from the null point at the 510 nm wavelength.

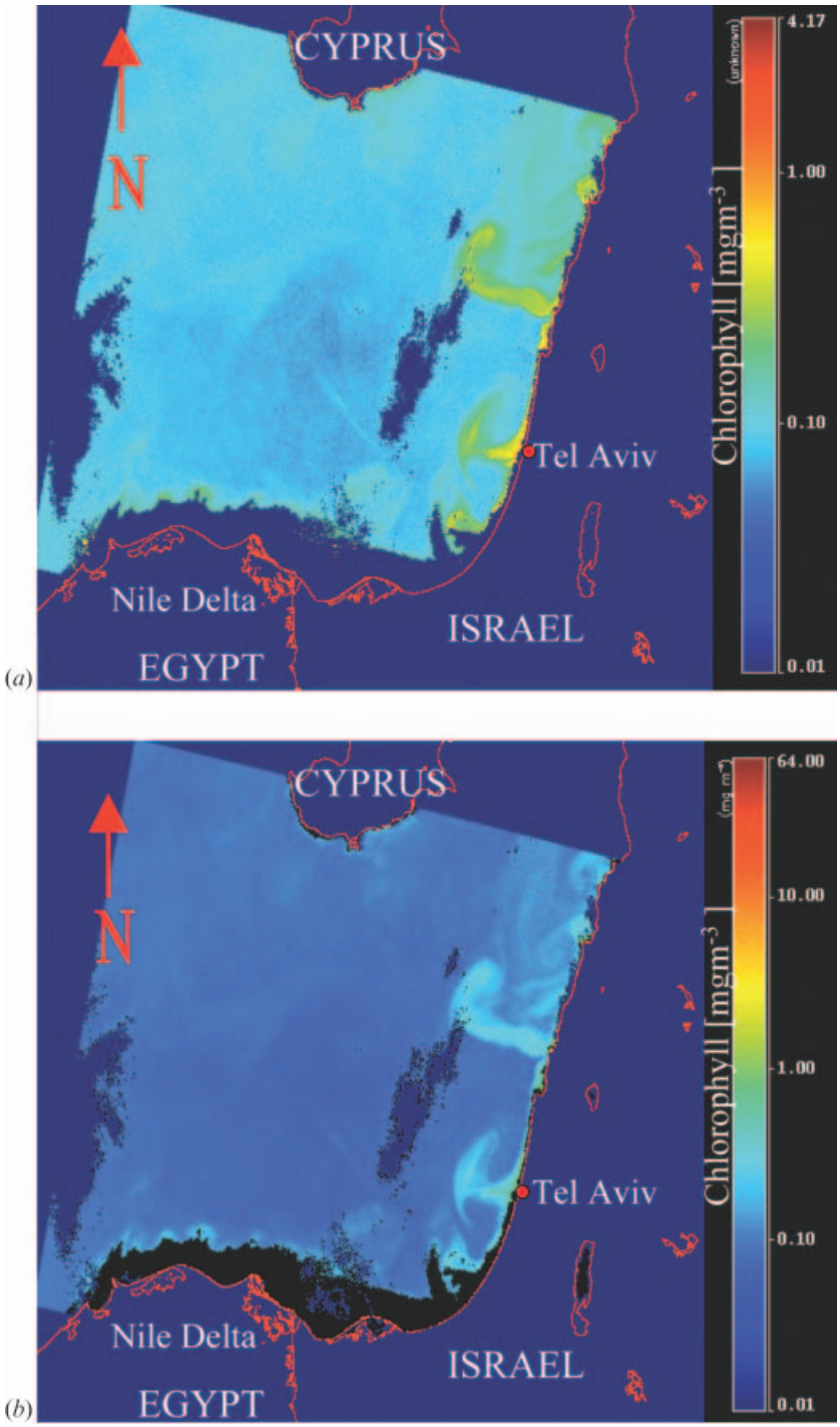

Figure 5. Turbid water mask models demonstrated on image of 18 June 2001 of the southeastern Mediterranean: (*a*) proposed procedure; (*b*) SeaDAS turbid water mask. Both models successfully mask the SM along the Egyptian coasts, however the current model is found to be more sensitive to CHL while their values are more reasonable (less than $1.00\,\mathrm{mg\,m^{-3}}$).

determining the normalized concentration (C_{caseII}) of SM in the area is:

$$C_{caseII} = \frac{R_{RS}510_{(caseII)} - (\sum_{i=1}^{m} R_{RS}510_{(caseI)})/m}{\max(R_{RS}510_{(caseII)} - (\sum_{i=1}^{m} R_{RS}510_{(caseI)})/m)} \quad (9)$$

where m is the number of pixels in the Case I sampling site.

A threshold value was implemented above the null point, at $R_{RS(510)} = 0.0055$. Figure 4 shows reflectance values of Case II water compared to those of Case I water. The Case II sediment-containing water's spectrum is higher than the threshold value. Operating the SeaDAS OC4V4 chlorophyll model in conjunction with this threshold and zeroing all pixels in the CHL model with values larger than the threshold results in masking of Case II water (figure 5(*a*)) as shown in the following model:

$$\text{IF} \quad (R_{RS}510_{(xi\,yi)} > 0.0055) \quad \text{THEN} \quad CHL_{(xi\,yi)} = 0.0$$

where *xi* and *yi* represent pixel coordinates. The SeaDAS turbid water mask is shown in figure 5(*b*) for comparison. Note the similarity between the two models in masking the SM belt along the Egyptian coasts. However, the current model was found to be more sensitive to CHL while the values are more reasonable (less than $1.00\,mg\,m^{-3}$).

7. Conclusions

1. The proposed procedure for detecting SM in water is a relatively simple and quick method, based on local concentrations of chlorophyll.
2. Applying the proposed procedure for masking SM produces results similar to the SeaDAS turbid water mask algorithm.
3. CHL concentrations in the proposed model are more clearly visualized than with the SeaDAS turbid water mask. The CHL values are presented within a realistic range.
4. Further research on results of this study, using the 510 nm spectral band as a reference, may lead to removal of turbid water effects on the spectrum without the need to zero the pixels and thus yield a closer-to-reality measure of chlorophyll concentrations in coastal areas, despite the presence of inorganic SM in the water. This may improve the monitoring of wastewater and sludge discharge in coastal areas, as well as pinpointing unauthorized discharge—an area of utmost importance.
5. The proposed method should be examined on other sensors having spectral bands for remote sensing of water, such as MODIS and MERIS.

References

BARGHAVA, D. S., and MARIAM, W., 1990, Spectral reflectance relationships to turbidity generated by different clay materials. *Photogrammetric Engineering and Remote Sensing*, **56**, 225–229.

BRICAUD, A., and MOREL, A., 1987, Atmospheric corrections and interpretation of marine radiances in CZCS imagery: use of a reflectance model. *Oceanologica Acta*, **7**, 33–50.

BUKATA, R. P., BRUTON, J. E., and JEROME, J. H., 1983, Use of chromaticity in remote measurements of water quality. *Remote Sensing of Environment*, **13**, 161–177.

BUKATA, R. P., JEROME, J. H., KONDRATYEV, K. Y., and POZDNYAKOV, D. V., 1995, The effects of chlorophyll, suspended minerals, and dissolved organic carbon on volume reflectance. In *Optical Properties and Remote Sensing of Inland and Coastal Waters* (Boca Raton, FL: CRC Press), pp. 135–166.

EMERY, K. O., and NEEV, D., 1970, Mediterranean beaches of Israel. *Geological Survey of Israel Bulletin*, **26**, 1–23.

FROIDEFONT, J. M., LAVENDER, S. J., LABORDE, P., HERBLAND, A., and LAFON, V., 2002, SeaWiFS data interpretation in a coastal area in the Bay of Biscay. *International Journal of Remote Sensing*, **23**, 881–904.

GITELSON, A., KARNIELI, A., GOLDMAN, N., YACOBI, Y. Z., and MAYO, M., 1996, Chlorophyll estimation in the Southeastern Mediterranean using CZCS images: adaptation of an algorithm and its validation. *Journal of Marine Systems*, **9**, 283–290.

HERUT, B., TIBOR, G., YACOBI, Y. Z., and KRESS, N., 1999, Synoptic measurements of chlorophyll-*a* and suspended particulate matter in a transitional zone from polluted to clean seawater utilizing airborne remote sensing and ground measurements, Haifa bay (SE Mediterranean). *Marine Pollution Bulletin*, **38**, 762–772.

KARNIELI, A., MAYO, M., GITELSON, A., and BEN-AVRAHAM, Z., 1993, Settlements in the Nile delta. *Systema Terra*, **2**, 49–50.

MCCLAIN, C. R., EVANS, R. H., BROWN, J. W., and DARZI, M., 1995, SeaWiFS quality control masks and flags: initial algorithms and implementation strategy. In *SeaWiFS Algorithms, Part I*, vol. 28, edited by S. B. Hooker, E. R. Firestone and G. Acker (Greenbelt, MD: NASA Goddard Space Flight Center), pp. 3–7.

MAYO, M., KARNIELI, A., GITELSON, A., and BEN AVRAHAM, Z., 1993, Determination of suspended sediment concentrations from CZCS data. *Photogrammetric Engineering and Remote Sensing*, **59**, 1265–1269.

MOREL, A., and PRIEUR, L., 1977, Analysis of variations in ocean colour. *Limnology and Oceanography*, **22**, 709–722.

NANU, L., 1993, The effect of suspended sediment depth distribution on coastal water spectral reflectance: theoretical simulation. *International Journal of Remote Sensing*, **14**, 225–239.

O'REILLY, J. E., and 24 co-authors, 2000, Ocean colour chlorophyll-a algorithms for SeaWiFS, OC2 and OC4: version 4. In *SeaWiFS Post Launch Calibration and Validation Analyses*, vol. 11, edited by S. B. Hooker and E. R. Firestone (Greenbelt, MD: NASA Goddard Space Flight Center), pp. 9–23.

TASSAN, S., 1981, A method for the retrieval of phytoplankton and suspended sediment concentrations from remote measurements of water colour. *Proceedings of the Fifteenth International Symposium on Remote Sensing of Environment* (Ann Arbor, MI: Environmental Research Institute of Michigan).